# Influence of Crystal Orientation on the Etch Rate and Crack Formation of Laser-modified Sapphire Using Ultrashort Pulsed NIR Laser Radiation

Christian Peters\*1, Jacqueline Blok1,2, Martin Kratz1, and Mehdi Behbahani2

<sup>1</sup>Fraunhofer ILT - Institute for Laser Technology, Steinbachstr. 15, 52074 Aachen, Germany <sup>2</sup>Biomaterials Laboratory, FH Aachen - University of Applied Sciences, Heinrich-Mussmann-Str. 1, 52428 Jülich, Germany

\*Corresponding author's e-mail: <u>christian.peters@ilt.fraunhofer.de</u>

Selective Laser-induced Etching (SLE) is a two-step laser process for the fabrication of precise 3D geometries from transparent dielectrics. Ultrashort pulsed near-infrared laser radiation is tightly focused to create modifications within the transparent material, which are subsequently removed in a wet chemical etching process. Due to its mechanical, optical, thermal and electrical properties Sapphire is of significant interest for a wide range of applications. However, its processing is challenging due to susceptibility to stress and crack formation. This study investigates the influence of different crystal orientations (C, A, M, R) on laser modification, crack formation and etch rate. Modifications are created in sapphire samples with different crystal orientations by variation of the pulse duration, pulse energy, pulse overlap and laser pulse repetition rate. Depending on the spatial and temporal energy deposition, three distinct modification regimes are identified. For low pulse energies (Regime I) the deposited energy is insufficient to generate continuous amorphous regions. The modifications are discontinuous, fragmented or intermittently absent and show negligible etch rates. For medium process energies (Regime II), homogeneous, stable modifications result in the highest etch rates (~35 μm/h for C/A, ~40 μm/h M/R) whereby excessive energy deposition (Regime III) leads to overprocessing of the material and reduced etchability. The findings indicate that a stable etch process requires a pulse overlap of 95-97% and while pulse duration does not significantly affect the etch rate pulse durations shorter than 1000 fs lead to reduced crack formation. The formation of micro cracks is highly crystal orientation dependent, with preferential propagation along the M-plane and is influenced by feed direction and repetition rate.

DOI: 10.2961/ilmn.2025.03.2012

Keywords: selective laser-induced etching, SLE, sapphire, crystal orientation

# 1. Introduction

The so-called Selective Laser-induced Etching (SLE) is a fabrication method to produce high-precision, three-dimensional components from transparent dielectrics. The SLE process is a two-step process. First, ultrashort pulsed (USP) near-infrared (NIR) laser radiation is tightly focused into a dielectric material. The high intensities achieved inside this focus volume (>10<sup>12</sup> W/cm<sup>2</sup>) trigger non-linear absorption effects (multi-photon absorption, tunnel ionization, etc.) and lead to an energy deposition of the photons inside the dielectric [1]. This leads to the formation of local in-volume modifications. By moving the laser focus selectively along previously calculated scanning vectors, large areas inside the transparent material can be modified. Depending on the selected laser parameters, the resulting modifications differ in their physical and chemical properties [2]. The induced modifications exhibit a higher etch rate to acids and alkalis. The second process step involves a wet chemical etching process in which the processed sample is exposed to an etchant in an ultrasonic bath. During the etching process, which lasts several hours, the modified areas are completely removed and the three-dimensional components are exposed. To enhance reactivity, the etchant is heated, and active ultrasound is applied. For the fabrication of complex

microstructures of micrometer precision, a high control of the tightly focus laser beam and process parameters such as pulse energy, pulse duration, repetition frequency, focus volume and corresponding intensity is required [3]. The SLE process has now been investigated for a variety of different materials such as fused silica [4-9], sapphire [10-12] and other glasses [13-18]. For fused silica in particular, the process has also been researched for a wide range of etching liquids and process parameters [19]. Selectivities of more than 1400:1 have been achieved for the SLE process with potassium hydroxide (KOH) [4]. Due to its outstanding optical, chemical, and mechanical properties, crystalline materials such as sapphire are attractive alternatives to established materials. Among other things, its high degree of hardness (9 on the Mohs scale), corrosion resistance (permanently corrosion-resistant), thermal stability (melting point at 2040 °C), biocompatibility and great electrical properties (breakdown voltage 48 kV/mm, dielectric loss factor 3 x 10<sup>-1</sup> 5) promise wide-ranging applications in medicine and (micro-) electronic technology [20-22]. Sapphire (Al<sub>2</sub>O<sub>3</sub>) is a variety of mineral corundum and, unlike glass, is a crystalline material with a trigonal crystal system and hexagonal crystal structure. It exhibits different crystal orientations (planes), which each have different physical properties,

making it suitable for a wide range of applications. [23–25]. The most common crystal orientations in sapphire are the C  $\{0001\}$ , A  $\{11\overline{2}0\}$ , M  $\{10\overline{1}0\}$ , and R  $\{1\overline{1}02\}$  planes. Figure 1 shows a crystallographic diagram of sapphire with the corresponding angles between these planes and their positions relative to each other.

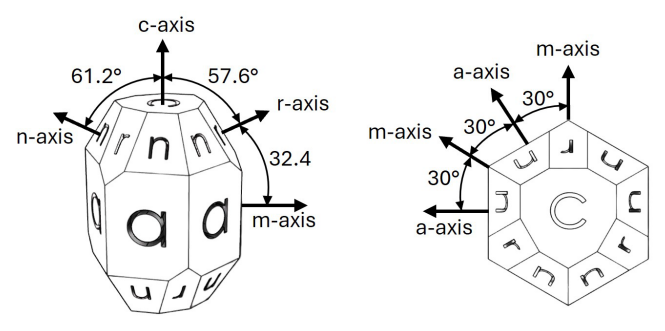


Fig. 1 Crystallographic diagram of sapphire. Based on [20].

Laser material processing of sapphire has already been investigated by many groups and is the subject of current research. Already in 2006, Gamaly et al. demonstrated that the modification in monocrystalline sapphire caused by ultrashort pulsed laser radiation is an amorphized state of sapphire, that exhibits increased chemical reactivity to acids and alkalis [26]. Since then, various research groups have demonstrated selectivities of over 1:10<sup>4</sup> [27,28]. Capuano et al. conducted a study on the influence of several (laser) process parameters on the formation of elongated structures in sapphire. The process window for the laser repetition rate determined in this study is between 0.1 and 1 MHz. In addition, a strong influence of the polarization used on the formation of modifications was observed [29]. Stankevič et al. investigated the etch rate as a function of double pulse irradiation and etching fluid of modified sapphire. It was shown that the combination of etching processes with 85 % H<sub>3</sub>PO<sub>4</sub>: 96 % H<sub>2</sub>SO<sub>4</sub> (3:1) and 40 % HF is suitable for etching modified sapphire and overcoming small recrystallized areas within the modifications. In addition, a higher etch rate was observed for A-oriented than for C-oriented sapphire [30]. Weng at al. have investigated the laser ablation of different orientated sapphire crystals. It has been shown that the defect formation and ablation volume correlate with different crystal orientations and the bonding layer between adjacent atomic layers [23].

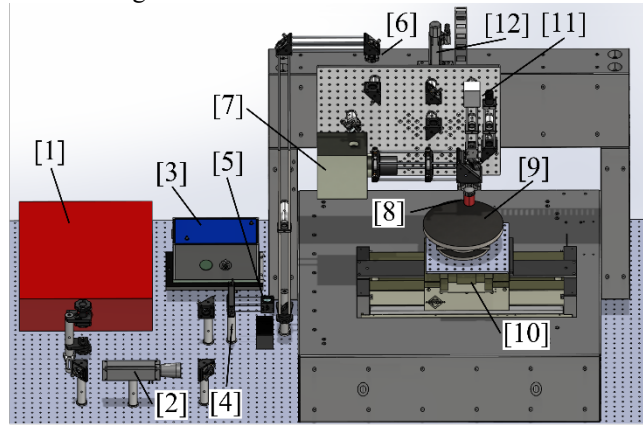
Despite high research efforts and the material properties that are advantageous for a wide range of applications, it is not yet possible to fabricate three-dimensional components from sapphire using the SLE process. Due to the crystalline structure sapphire is sensitive regarding stress and crack formation. Laser structuring using tightly focusing optics leads to the formation of sustainable modifications with different material properties than the surrounding pristine material. Predominantly the change of density is what leads to the formation of shockwaves and lasting stress inside the sapphire crystal, which is released in the form of cracks. The fabrication of complex (3D) geometries using the SLE process requires a better understanding of laser-material interactions as well as laser-induced damage. However, the crystal orientation-dependent etch rate and crack formation have not been investigated yet. To overcome this scientific gap, we investigate the influence of different crystal orientations (C, A, M, R) on laser modification, crack formation and etch

rate, with the objective of advancing the SLE process for sapphire.

Chapter 2 describes the experimental setup and method, including the process parameters evaluated. Chapter 3.1 provides an overview of the crystal orientation-dependent etch rate of monocrystalline sapphire. The process parameters are classified into different modification regimes and their influence on the etch rate is discussed. Chapter 3.2 focuses on the crystal orientation-dependent microcrack formation of laser-modified and etched sapphire. Based on the results, a TWV demonstrator with a minimum hole diameter is manufactured using SLE. A critical evaluation and a summary of the results are provided in Chapter 4.

### 2. Materials and Experimental setup

A schematic illustration of the experimental setup is shown in Figure 2.



- [1] USP laser source [5] Pol. beamsplitter [9] Chuck
- [2] Telescope [6]  $\lambda/4$  plate [10] x-y-Axis
- [3] Autocorrelator [7] Scanner [11] Camera
- [4] λ/2 plate [8] Objective [12] z-Axis **Fig. 2** Schematic illustration of the experimental setup.

The USP laser source used to carry out the experiments is the Trumpf TruMicro2000 system. This laser emits light of wavelength  $\lambda = 1030$  nm,  $M^2 < 1.2$  with an average power of up to P = 20 W at repetition rates from single pulse to  $f_{Rep} = 1$  MHz and pulse durations between  $\tau = 380$  fs to 10 ps. The raw beam diameter is expanded to  $d_{raw} = 6$  mm with the aid of a telescope. This is then followed by a beam splitter and quarter-wave plate to generate circular polarized light. Due to the known influence of polarization on etch rate and formation of nanogratings, only circularly polarized light is used during the experiments [2]. The polarization plate is followed by a microscanner system consisting of a galvanometer scanner (SCANLAB intelliSCANse 14) and focusing optic (Mitutoyo M Plan Apo NIR 20x/0.4). Beam caustic measurements are performed to experimentally determine the minimum focus diameter. The beam profile is recorded in multiple z-planes around the focal plane and analyzed with respect to the beam radius by fitting a Gaussian beam profile to the cross sections. The minimum focus diameter determined this way is 3.52 µm. The optical components including the scanner system are mounted on a mechanically supported linear stage (Aerotech Pro165LM). Below the focusing optics, a sample holder is mounted on an air-bearing axis system (Aerotech Pro225 and Pro115). With the aid of an alignment stage the sample material is aligned to the

focusing optics with micrometer precision. In this work,  $100 \text{ mm} \times 60 \text{ mm} \ (\pm 0.3 \text{ mm}) \ \text{and} \ 4 \text{ mm} \ (\pm 25 \text{ }\mu\text{m}) \ \text{thick}$  double-sided polished (Ra < 3 nm) sapphire sample material with the crystal orientations C, M, R, and A (hereinafter referred to as C-, M-, R- and A-sapphire) with a purity of > 99.98 % from Siegert Wafer GmbH is used.

A parameter study is carried out to determine the process parameters and crystal orientation-dependent etch rate of laser-modified sapphire. For this purpose, modification lines are structured in sapphire at a sample depth of 200  $\mu$ m using an experimental setup shown in Figure 2 and summarized in table 1.

**Table 1** Process parameters used for this study.

Parameter	Value
Wavelength	1030 nm
Focus diameter	3.52 µm
Objective NA	0.4
Polarization	circular
Etching liquid	HF
HF concentration	48 %
Etching temperature	85 °C
Etch duration	24 h
Ultrasonic frequency	35 kHz
Crystall orientation	C-, A-, M- & R-sapphire

The modification lines are structured using only the mechanical stages and without the scanner. An overview of the parameters processed in this work is summarized in the following table 2. The different pulse overlaps for a constant repetition frequency are adjusted by changing the feed velocity of the laser. The formula for the calculation is well known in the literature and can be found, for example, in [31].

**Table 2** Process parameters varied during parameter study.

Parameter	Value
Pulse energy	0.1 μJ - 1 μJ (0.1 μJ steps) 1 μJ - 3 μJ (0.25 μJ steps)
Repetition rate	125 kHz, 250 kHz, 500 kHz, 1000 kHz
Pulse overlap (see [31])	90 %, 95 %, 97 %, 99 %
Pulse duration	380 fs, 700 fs, 1000 fs
Feed speed	4.4 - 176 mm/s

A total of six modification lines, three for each direction, are structured and evaluated for each parameter combination.

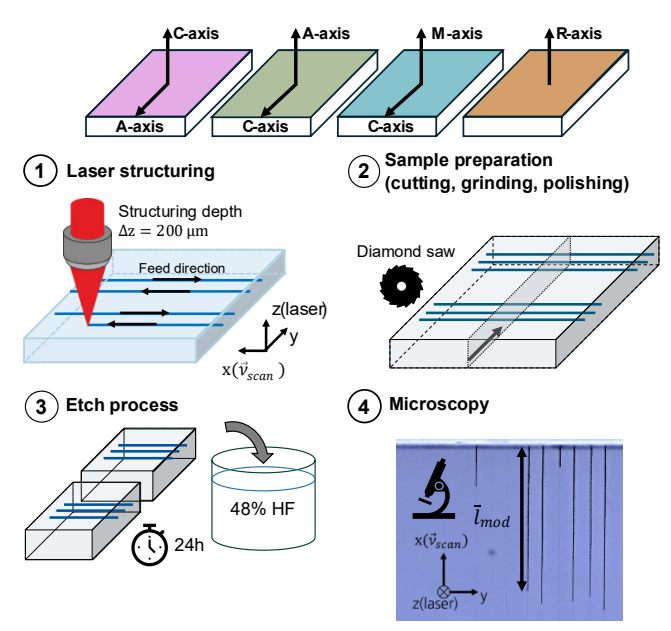


Fig. 3 Schematic illustration of sample preparation.

The sample alignment shown in Figure 3 (top) is used during the laser structuring process the same way as illustrated in step 1. After laser structuring, the sample material is cut using a diamond band saw. The interfaces are ground and polished, then etched for 24 hours in 48 % hydrofluoric acid (ARISTAR®,  $HYDROFLUORIC\ ACID\ 48\ \%$ ). The modification and etch channels are evaluated using optical microscopy (Keyence  $VHX\ 6000$ ). One quantifiable variable to determine the etch ability of modified material is the etch rate  $\bar{\Gamma}_{mod}$ :

$$\bar{\mathbf{r}}_{\mathbf{mod}} = \frac{\bar{\mathbf{l}}_{\mathbf{mod}}}{\mathbf{t}_{\mathbf{etch}}} \,. \tag{1}$$

The etch rate  $\bar{r}_{mod}$  [ $\mu m/h$ ] is the ratio of etch channel length  $\bar{l}_{mod}$  [ $\mu m$ ] divided by the etch duration  $t_{etch}$  [h]. This equation does not consider the etch rate of the pristine material. Since the etch rate of crystalline material is < 0.1  $\mu m/h$  the sample plate fabrication tolerance and waviness is greater than the measurable sample thickness differences after a total etch duration of 24 h and was therefore not considered to calculate selectivities [32].

#### 3. Results

## 3.1 Crystall orientation dependent etch rates

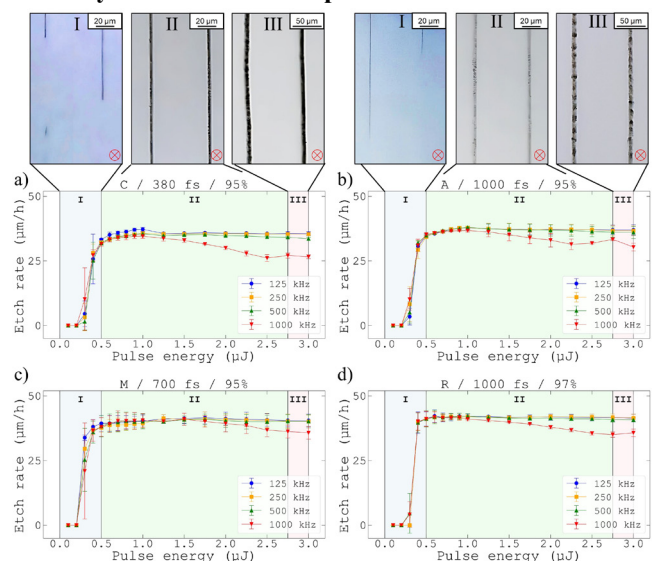


Fig. 4 Etch rate over pulse energy for different repetition rates with color-coded modification regimes (I: blue, II: green, III: red). a) C-sapphire, 380 fs, 95 % with microscopy image of modification lines, b) A-sapphire, 1000 fs, 95 % with microscopy image of modification lines, c) M-sapphire, 700 fs, 95 %, d) R-sapphire, 1000 fs, 97 %

Figure 4 shows the characteristic curves for the etch rate as a function of pulse energy for different repetition rates and crystal orientations. The pulse duration and pulse overlap are selected in such a way that the most stable process windows, regarding consistently high etch rates, are shown for each crystal orientation. The curve can be divided into three modification regimes with regard to the properties of the modification lines. These transitions are gradual rather than abrupt, and in practice the regimes may partially overlap:

- Modification Regime I covers the pulse energy range up to the consistent modification threshold value. These values lie between pulse energies of 0.2–0.5 μJ. In this regime, intensities below and above the absorption threshold but below the threshold for the creation of sustainable modifications are reached [12,26,33]. Thus, modification lines are either absent or appear inhomogeneous and fragmented, often interrupted by regions of unmodified crystalline material, as shown in the microscopy image in Figure 4 (Modification Regime I). Due to the vanishing etch rate of crystalline sapphire, the unmodified areas act as a barrier to the etching fluid. This results in no measurable or strongly varying etch channel lengths (high error bars).
- With increasing pulse energy, the modification becomes homogeneous and stable. The etch channels show low variation in etch channel length, resulting in the highest measurable etch rates. This region, characterized by uniform modifications and consistent etch rates, is defined as Modification Regime II.
- In Modification Regime III, the energy deposition into the material increases as a result of increasing pulse energy. Critical thresholds are exceeded,

particularly at high repetition rates, which increasingly leads to the formation of an inhomogeneous modification pattern, possibly voids, which has a negative effect on etchability and leads to lower etch rates

The modification threshold of approximately 0.5  $\mu$ J (380 fs) equivalent to 2.54·10<sup>13</sup> W/cm<sup>2</sup> is one order of magnitude lower than the value Capuano et al. have found with a modification threshold intensity of 2.5·10<sup>14</sup>  $\pm$  0.4·10<sup>14</sup> W/cm<sup>2</sup> [34]. The average etch rates in Regime II are approximately 35  $\mu$ m/h for C-/A-plane sapphire and 40  $\mu$ m/h for M-/R-plane sapphire. The maximum measured etch rate is 42  $\mu$ m/h, which is in good agreement with Butkutè et al., who reported an etch rate of < 50  $\mu$ m/h for amorphized C orientated sapphire etched in 48 % HF [32].

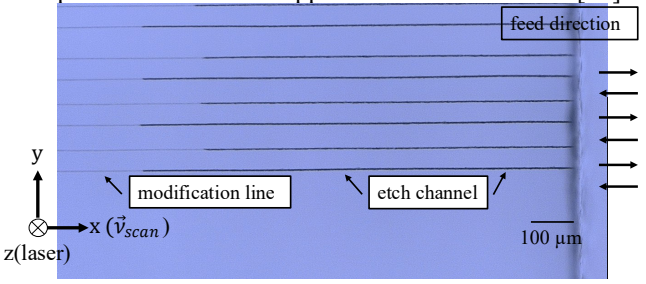


Fig. 5 Microscopy image of feed directional dependent etch rate. Process parameters: R-sapphire, 380 fs, 500 kHz, 95 %, 1 μJ

After the etching process, a correlation between the etch channel length and the feed direction of the laser is visible. Figure 5 shows an example of a microscope image from an exemplary parameter set in which the laser structuring direction is reversed between each modification line. The direction-dependent etch channel length difference is noticeable for all crystal orientations and process parameters and amounts to up to 20 % of the total etch channel length. However, the effect is greatest for M- and R-sapphire crystal orientations. This effect is well known from the laser structuring and etching of fused silica and probably caused by the pulse front tilt of the laser beam [35].

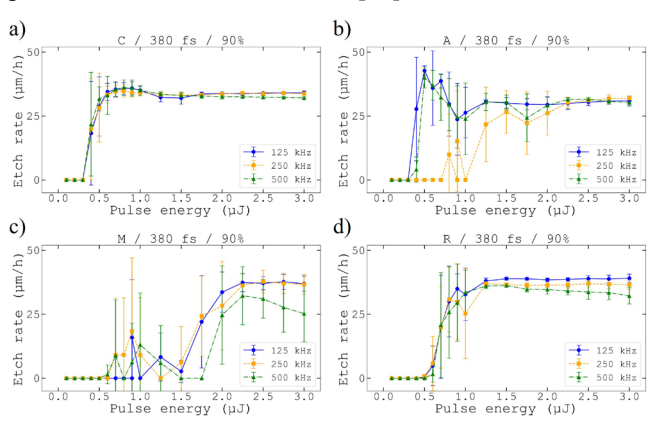


Fig. 6 Etch rate over pulse energy for different repetition rates, 380 fs and 90 %. a) C-sapphire, b) A-sapphire, c) M-sapphire, d) R-sapphire

Figure 6 shows the etch rate as a function of pulse energy and repetition frequency for a pulse overlap of 90 %. Due to the negligible etch rate of crystalline sapphire, a homogeneous modification line is essential for a stable process window with high etch rates. A pulse overlap of 90 % therefore

represents the lower threshold value for the generation of homogeneous modification lines. The graphs show that the influence of the repetition rate within the process window defined by Capuano et al. of 0.1–1 MHz has no significant influence on the amorphization process of sapphire and thus on the etch rate. Overall, higher pulse energies are required for A- and M-sapphire to create sustainable homogeneous modification lines. The range of process parameters from modification regime II is significantly lower than for C- and R-sapphire. A possible explanation for the lower pulse energy required to create homogeneous modification lines are the weakened Al-Al and O-O bonds, which are increasingly found in the C and R planes. For Al-Al bonds the linear expansion coefficient is highest within the sapphire crystal (17.5 · 10<sup>-6</sup> °C<sup>-1</sup>). During the laser structuring the implemented heat leads to separation of single atoms and destruction of atomic bonds. Thus, Al-Al bonds are easier to break than Al-O not only chemically, but also mechanically [20]. For the R-plane, the bonds between the O-O layers at a distance of 1.06 Å are weakened [20]. It is therefore easier during the laser structuring process to break these bonds. Creating an amorphized state of sapphire within these crystal orientations (C- and R-sapphire) requires less energy and leads to wider process windows with more stable etch rates.

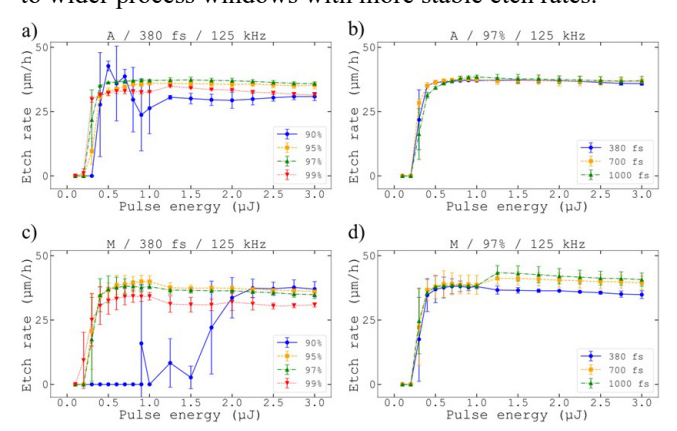


Fig. 7 Etch rate over pulse energy for different pulse overlaps (a) A-sapphire, 380 fs, 125 kHz and c) M-sapphire, 380 fs, 125 kHz) or pulse duration (b) A-sapphire, 97 %, 125 kHz and d) M-sapphire, 97 %, 125 kHz).

Figure 7 shows the etch rate as a function of pulse energy and pulse overlap (left side) and pulse duration (right side) for the crystal orientations A and M. For a pulse overlap of 90%, both crystal orientations exhibit unstable etch rates since low pulse overlaps lead to regular process interruptions. The modification line is interrupted by pristine, crystalline areas (modification regime I), which lead to unstable etch rates as discussed above. A pulse overlap of 99 % leads to structures of modification regime III, especially for higher pulse energies and pulse repetition frequencies. In this case, the energy input exceeds a critical threshold value and leads to the formation of inhomogeneous modification patterns, which have a negative effect on the etch rate (see Figure 4). A pulse overlap of 95 % and 97 % leads to homogeneous modification lines and stable etch rates. These observations are shown in Figure 7 exemplary for crystal orientations A and M, but can also be observed for crystal orientations C and R. Two potential mechanisms are proposed to account the observed phenomena. With increasing pulse overlap, the deposited energy per unit length and the temperature

increases. High temperatures of several thousand Kelvin lead to dissociation of oxygen. Due to the higher mobility and the strong bond of oxygen molecules in combination with the rapid cooling due to high thermal gradients in the modification volume, (gas) voids are formed which occur as inhomogeneous modification patterns. This process is analogous to the formation of gas bubbles in fused silica subjected to high repetition rate pulse laser irradiation [36–38]. For decreasing pulse overlap und thus decreasing temperature the conditions for oxygen formation vanish. The second approach considers void formation as resulting from extreme pressure conditions within the laser focal volume and is well explained by Gamaly et al.. When the local pressure exceeds the material's Young's modulus, structural failure can occur. In the case of sapphire (Young's modulus ~ 400 GPa) voids may form when pressure in the order of 2.6 TPa is generated by the micro explosions and rapid material compression that follows the absorption of a highintensity laser pulse (I >  $10^{14}$  W/cm<sup>2</sup>) [12,26]. Which of the two proposed explanations are primarily responsible for the observed modification pattern/void formation is unclear and requires further investigation.

Figure 7 also shows that the pulse duration has no significant influence on the etch rate. All pulse durations (380 fs, 700 fs, and 1000 fs) lead to similar stable etch rates within modification regime II. Significant differences in the laser structuring of sapphire with different pulse durations can be observed in the formation of stress and cracks. A long pulse duration of 1000 fs leads to significantly increased formation of stresses and cracks compared to 380 fs and 700 fs. Figure 8 shows a cross-section of a total of 6 modification lines in A- oriented sapphire.

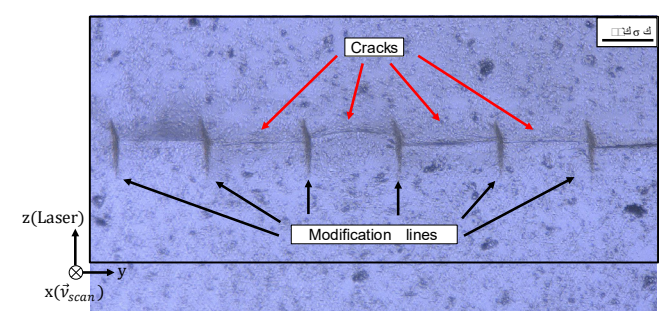


Fig. 8 Crosssection of modification lines with (macro) cracks. Process parameters: A-sapphire, 1000 fs, 125 kHz, 97 %, 3 μJ

Cracks are observed between the modification lines. In this study, this type of cracking (macro cracks) is observed exclusively for a pulse duration of 1000 fs. This behavior is attributed to the shift towards a more avalanche ionization dominated absorption mechanism for longer pulse durations and high intensities [1,39]. Due to the avalanche ionization process, the energy deposition increases resulting in increased heat. This leads to high temperature gradients within the effective range of the laser focus, which in turn induces stresses that are relieved in cracks. These cracks follow the path of least resistance and are therefore formed between the individual modification lines. For laser structuring of complex, interconnected modification areas as part of the SLE process, shorter pulses < 700 fs are therefore recommended.

# 3.2 Crystall orientation dependent formation of micro cracks

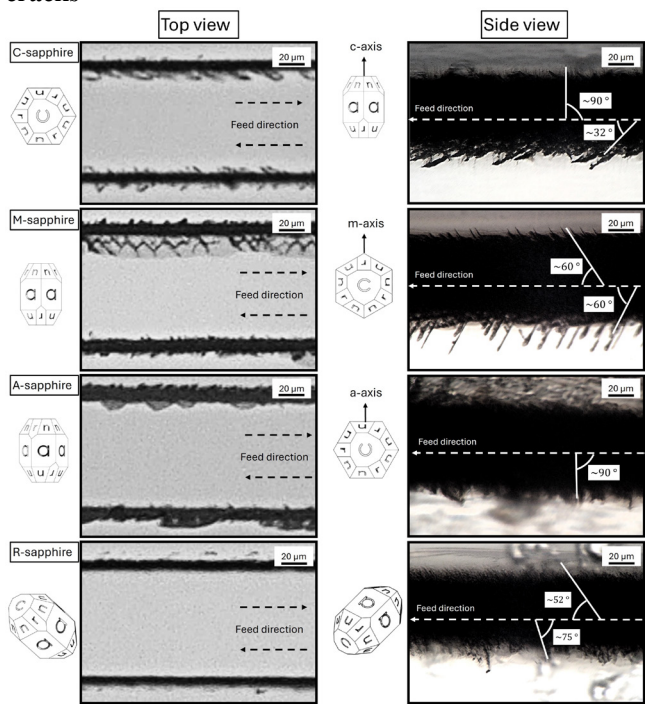


Fig. 9 Microscopy images of etch channels in different sapphire crystal orientations (left) top view, (right) side view and corresponding crystallographic diagram. Process parameters: 1000 fs, 125 kHz, 3 μJ

As a result of the stress induced during laser structuring, cracks form along the modification line. Figure 9 shows the crack formation, depending on the crystal orientation along the etch channels from two different perspectives (top view, side view). In addition, the crystallographic diagram is shown, which is aligned according to the observer's viewing perspective. The planes shown in the crystallographic diagram are therefore aligned identically to the crystal planes of the sapphire sample shown in the microscopy image. For all crystal orientations, a clear formation of microcracks is visible after the structuring and etching process. With increasing pulse duration, pulse overlap, and pulse energy, crack formation increases. The visible microcrack formation increases with decreasing repetition rate in this study. Lower repetition rates such as 125 kHz lead to a significantly higher density and overall longer microcracks. Our hypothesis for this behavior is an alternating melting and solidification regime. Due to the high thermal conduction of sapphire compared to glasses the melt zone which leads to absorption after an incident pulse solidifies. These alternating processes lead to less relaxation of the heated material as in the case of high repetition rates and thus to increased stress and cracks. To verify this hypothesis, in situ measurements with a highspeed camera or pump-probe microscopy are necessary.

On the left side of Figure 9, a microscopic image taken from a top view is shown for each crystal orientation, revealing two etch channels that were structured in different feed directions. For all crystal orientations, a clear correlation between the preferred direction of crack propagation and the feed direction of the laser can be observed. The crack propagation tends to run in the direction of the laser structuring. The density and periodicity of microcrack propagation

varies between the different crystal orientations. C, M, and A sapphire show significant crack formation along the etch channel, whereas R sapphire exhibits a lower density but more pronounced, longer cracks. The etch channel for M and A sapphire is significantly wider than for C and R sapphire and shows visible stress and cracks perpendicular to the feed and beam direction. These stress and crack affected zones run parallel to the respective crystal plane in a horizontal direction and are either visible as breakouts at the edge of the etch channel or as a change in the refractive index as a result of stress birefringence. The right-hand side of Figure 9 shows microscopic images of cross-polished sections of the individual etch channel (side view). The images show the propagation of microcracks in a vertical direction, perpendicular to the processed crystal orientation and in parallel to the laser beam. Once again, the formation of microcracks is visible for all crystal orientations. The microcracks also form periodically and in a uniform direction. Thus, the angle between the crack propagation and the etch channel is analyzed. Crystal orientation C shows crack propagation at 90° and 32° relative to the structuring direction. With regard to the crack formation visible in the top view and the angle specifications between the individual crystal planes, illustrated in the crystallographic diagram (Figure 1), crack propagation occurs preferentially along the M (90°) and R (32.4°) planes. For M- and A-sapphire an angle of 60° (Msapphire) and 90° (A-sapphire) was measured. The crack propagation for these two crystal orientations therefore also occurs preferentially along the M crystal plane. For the angles of 52° and 75°, measured for R sapphire, no clear crystal plane could be identified. Due to the special position of the plane within the unit cell, further measurements, possibly using micro-CT, are necessary to gain a better three-dimensional understanding of the crack propagation. For the C-, A- and M- orientated sapphire a preferred crack propagation along the M-plane can be observed. Wen et al. found similar results for crack formation and propagation in laser ablation experiments. The calculated and experimental verified data showed that laser damage accumulation is greater for the M plane than for the other planes, indicating that the thermal stress is greatest in the M plane. Therefore, during the usp laser material interaction, the M-plane is more susceptible to the formation of cracks than the other crystal orientations [24,40]. However, additional experiments and further investigations are needed to verify this hypothesis.

One of the biggest challenges in processing monocrystalline sapphire using the SLE process is the formation of stress and cracks during laser structuring. Even simple 2.5D geometries such as through wafer vias (TWVs) for the fabrication of circuit boards in high-performance electronics or for through-hole plating pose a major challenge when producing holes with small diameters < 1 mm. Based on the results of this work, a crystal orientation is specifically selected that enhances crack propagation along the modification plane. This is intended to counteract damage and crack formation perpendicular to the TWVs. For A-sapphire Figure 8 shows a crack propagation with an orientation of 90° to the sample surface. As part of the SLE process modification lines are created within the sample material along the surface of the cylindric hole (TWV). When using A-sapphire, microcrack propagation occurs along the outer surface and compared to the crystal orientations C, R, and M sapphire,

barely or to a negligible extent in the horizontal (parallel to the crystal plane) direction. Using this procedure, various hole diameters (1000  $\mu$ m, 500  $\mu$ m, 250  $\mu$ m) are structured within A-oriented 430  $\mu$ m thick sapphire samples and etched for 72 hours in 48 % HF.

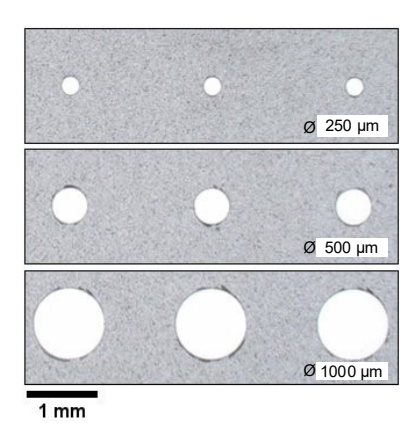


Fig. 10 Microscopy images of TWVs with different hole diameters (1000  $\mu$ m, 500  $\mu$ m, 250  $\mu$ m) in A-sapphire. Process parameters: 380 fs, 500 kHz, 1  $\mu$ J, 99 %, 24 h etched in 48 % HF

The microscopic image in Figure 10 shows TWVs with different hole diameters and minimal/no crack formation after etching in HF. Compared to other crystal orientations, crack formation was significantly reduced, and the small hole diameters (250  $\mu$ m) are produced without any visible damages.

#### 4. Conclusion

This work shows the influence of crystal orientation on the etch rate and (micro-) crack formation of laser-modified sapphire. Using a highly focused USP NIR laser, modification lines are structured in differently oriented sapphire samples (C, A, M, R) by varying the pulse duration, pulse repetition rate, pulse overlap, and pulse energy, and then etched in 48 % HF for 24 hours. Depending on the modification characteristics and the resulting etch rate, three modification regimes (I, II, and III) are identified. Crystal orientations C and R proved to be stable with respect to process parameter variations and exhibited stable etch rates even in the process parameter limits investigated in this study. Etch rates of > 38 µm/h are archived for all orientations. With higher energy deposition as a result of increasing pulse energy and repetition rate, the formation of inhomogeneous modification pattern is observed. No influence of the pulse duration on the etch rate is found but longer pulse durations lead to increased crack formation. The etch rate is sensitive to variations in pulse overlap. Low pulse overlap leads to increased modifications of Regime I, and excessive pulse overlap leads to modifications of Regime III, resulting in process interruptions and unstable etch rates. The most stable etch rates are achieved with a pulse overlap of 95 % and 97 %.

For all crystal orientations, the formation of microcracks along the modification line could be observed. These occur periodically and at a fixed angle along the modification line and in the laser structuring direction. The cracks form preferentially along the M plane. Why this crystal plane is particularly susceptible to crack formation cannot be clarified and requires further investigation. For A- oriented sapphire, a preferred crack propagation occurs at 90° to the laser

modification, parallel to both the laser beam and the TWV wall, while minimal crack propagation is observed in the horizontal direction. Based on these fundamental results, the SLE fabrication of crack-free TWVs in 430 µm thick wafers with a minimum hole diameter of 250 µm is demonstrated.

#### References

- [1] C. Kalupka: "Energiedeposition von ultrakurz gepulster Laserstrahlung in Gläsern", Dissertation, (Apprimus Verlag, RWTH Aachen University, 2019) p.6.
- [2] R. S. Taylor, C. Hnatovsky, and E. Simova: Laser Photonics Rev., 2, (2008) 26.
- [3] M. Kratz, L. Rückle, C. Kalupka, M. Reininghaus, and C. L. Haefner: Opt. Express, 31, (2023) 26104.
- [4] J. Gottmann, M. Hermans, N. Repiev, and J. Ortmann: Micromachines, 8, (2017) 110.
- [5] M. Hermans, J. Gottmann, and F. Riedel: J. Laser Micro Nanoeng., 9, (2014) 126.
- [6] A. Butkutė, T. Baravykas, J. Stančikas, T. Tičkūnas, R. Vargalis, D. Paipulas, V. Sirutkaitis, and L. Jonušauskas: Opt. Express, 29, (2021) 23487.
- [7] S. Kim, J. Kim, Y.-H. Joung, S. Ahn, J. Choi, and C. Koo: Micro and Nano Syst. Lett., 7, (2019) 15.
- [8] C. Peters, M. Kratz, J. Köller, S. Borzek, and S. Simeth: Proc. SPIE, Vol. 12873, (2024) 1.
- [9] C. Peters, B. Geppert, E. Dashjav, M. Kratz, and F. Tietz: J. Laser Micro Nanoeng., 19, (2024) 85.
- [10] M. Hörstmann-Jungemann, J. Gottmann, and M. Keggenhoff: J. Laser Micro Nanoeng., 5, (2010) 145.
- [11] M. Hörstmann-Jungemann, J. Gottmann, and D. Wortmann: J. Laser Micro Nanoeng., 4, (2009) 135.
- [12] L. Capuano: "Laser micro/nanoprocessing and subsequent chemical etching of sapphire for surface and bulk functionalization", Dissertation, (Ipskamp Printing, University of Twente, 2020) p.84.
- [13] D. Bischof, M. Kahl, and M. Michler: Opt. Mater. Express, 11, (2021) 1185.
- [14] A. Crespi, Roberto Osellame, and F. Bragheri: Opt. Mater., 4, (2019) 1.
- [15] R. Memeo, M. Bertaso, R. Osellame, F. Bragheri, and A. Crespi: Appl. Sci., 12, (2022) 948.
- [16] S. Bang, G. Asghar, J. Hwang, K. S. Lee, W. Jung, K. Mishchik, H. Kim, and K.-G. Lee: Opt. Express, 33, (2025) 3214.
- [17] H. Yao, Q. Xie, M. Cavillon, Y. Dai, and M. Lancry: Progress in Materials Science, 142, (2024) 101226.
- [18] M. Kratz, J. Köller, J. Theis, and O. Hofmann: Proc. SPIE, Vol. 12873, (2024) 1287304.
- [19] E. Casamenti, S. Pollonghini, and Y. Bellouard: Opt. Express, 29, (2021) 35054.
- [20] V. Pishchik, L. A. Lytvynov, and E. R. Dobrovinskaya: "Sapphire" (Springer, Boston, MA, 2009) p.1.
- [21] Klein & Becker, "Eigenschaften von Saphir", http://www.klein-becker.com/files/downloads/Eigenschaften%20Saphir.pdf (Accessed 27 August 2025).
- [22] L. Geng and H. Yihong: Cryst. Res. Technol., 53, (2018) 1.
- [23] Q. Wen, P. Zhang, G. Cheng, F. Jiang, and X. Lu: Ceram. Int., 45, (2019) 23501.

- [24] K. Wang, F. Jiang, L. Yan, X. Xu, N. Wang, X. Zha, X. Lu, and Q. Wen: Ceram. Int., 45, (2019) 7359.
- [25] A. Montagne, S. Pathak, X. Maeder, and J. Michler: Ceram. Int., 40, (2014) 2083.
- [26] E. G. Gamaly, S. Juodkazis, K. Nishimura, H. Misawa, B. Luther-Davies, L. Hallo, P. Nicolai, and V. T. Tikhonchuk: Phys. Rev. B, 73, (2006) 1.
- [27] S. Juodkazis, K. Nishimura, H. Misawa, T. Ebisui, R. Waki, S. Matsuo, and T. Okada: Adv. Mater., 18, (2006) 1361.
- [28] D. Wortmann, J. Gottmann, N. Brandt, and H. Horn-Scholle: Opt. Express, 16, (2008) 1517.
- [29] L. Capuano, R. M. Tiggelaar, J. W. Berenschot, J. G. E. Gardeniers, and G. R. B. E. Römer: Opt. Lasers Eng., 133, (2020) 106114.
- [30] V. Stankevič, J. Karosas, R. Gvozdaitė, G. Račiukaitis, and P. Gečys: Opt. Laser Technol., 167, (2023) 109620.
- [31] J.-T. Finger: "Puls-zu-Puls-Wechselwirkungen beim Ultrakurzpuls-Laserabtrag mit hohen Repetitionsraten", Dissertation, (Apprimus Verlag, RWTH Aachen University, 2017) p.31.
- [32] A. Butkutė, R. Sirutkaitis, D. Gailevičius, D. Paipulas, and V. Sirutkaitis: Micromachines, 14, (2022) 1.
- [33] D. von der Linde and H. Schüler: J. Opt. Soc. Am. B, 13, (1996) 216.
- [34] L. Capuano, R. Pohl, R. M. Tiggelaar, J. W. Berenschot, J. G. E. Gardeniers, and G. R. B. E. Römer: Opt. Express, 26, (2018) 29283.
- [35] P. G. Kazansky, M. Beresna, Y. Shimotsuma, K. Hirao, and Y. P. Svirko: Proc. SPIE, Vol. 7600, (2010) 760017.
- [36] Y. Bellouard and M.-O. Hongler: Opt. Express, 19, (2011) 6807.
- [37] S. Richter, S. Döring, F. Burmeister, F. Zimmermann, A. Tünnermann, and S. Nolte: Opt. Express, 21, (2013) 15452.
- [38] K. Cvecek, I. Miyamoto, and M. Schmidt: Opt. Express, 22, (2014) 15877.
- [39] B. Rethfeld: Phys. Rev. B, 73, (2006) 1.
- [40] Y. Jee, M. F. Becker, and R. M. Walser: J. Opt. Soc. Am. B, 5, (1988) 648.

(Received: July 12, 2025, Accepted: October 25, 2025)